Positron-surface sticking rates

Alison B. Walker and Kjeld O. Jensen
School of Physics, University of East Anglia, Norwich NR4 7TJ, United Kingdom

J. Szymański
Telecom Australia Research Laboratories, 770 Blackburn Road, Clayton, Victoria 3168, Australia

D. Neilson
School of Physics, University of New South Wales, Kensington, Sydney 2033, Australia
(Received 17 June 1991)

The probability that positrons are trapped into the image-potential-induced state on a metal surface, i.e., "stick" to the surface, is discussed. Our model assumes that the positrons couple weakly to the surface and, hence, that the sticking coefficient goes to zero as the temperature tends to zero. This assumption is validated by the order-of-magnitude agreement with experimental data that we obtain for trapping rates for thermalized and epithermal positrons. We have also predicted that the trapping rate varies strongly with the positron work function and that trapping rates into helium bubbles are significantly smaller than for empty cavities.

I. INTRODUCTION

There has recently been renewed interest in the role of quantum effects in the behavior of particles near a solid or liquid surface[1–4] especially with reference to electrons on the surface of liquid He. A quantum particle sticks to the surface by forming a bound state in a surface potential well. As the temperature T of a quantum particle of mass m tends to zero, the particle will be reflected off a rigid surface since its de Broglie wavelength ($=\hbar\sqrt{2\pi/mk_BT}$; k_B is Boltzmann's constant) becomes so large that there is a vanishingly small overlap with the well.[5] However, it has been argued[3] that the sticking probability for quantum particles at low temperatures will tend to unity if the particle-surface coupling is sufficiently strong that the surface is modified by the particle-surface interactions and so is no longer rigid. Determining the strength of the coupling and the value that determines the crossover between the two cases is a subject of much debate.

Positrons provide an interesting example of quantum particles that may stick to surfaces. Figure 1 illustrates the processes that occur prior to and after implantation of a positron into a surface. On entering the surface, positrons may be trapped in the image-potential-induced well or, once implanted, those that return to the surface may be trapped. Britton *et al.*[6] and Huttunen *et al.*[7] have recently made experimental measurements on positron-surface interactions for metals at low temperatures. In these experiments, keV positrons are implanted into a solid where they rapidly thermalize. Some of the positrons diffuse back to the surface where several channels become available to the emerging positron: emission as a free positron, emission as positronium, Ps (which can only form outside the surface of a metal or semiconductor where the electron density is sufficiently small), and trapping into the surface state induced by the image potential.

In Refs. 6 and 7 the results clearly show that thermal positron and Ps fluxes at clean Cu(111), Al(110), and Ag(111) surfaces are strongly reduced at low tempera-

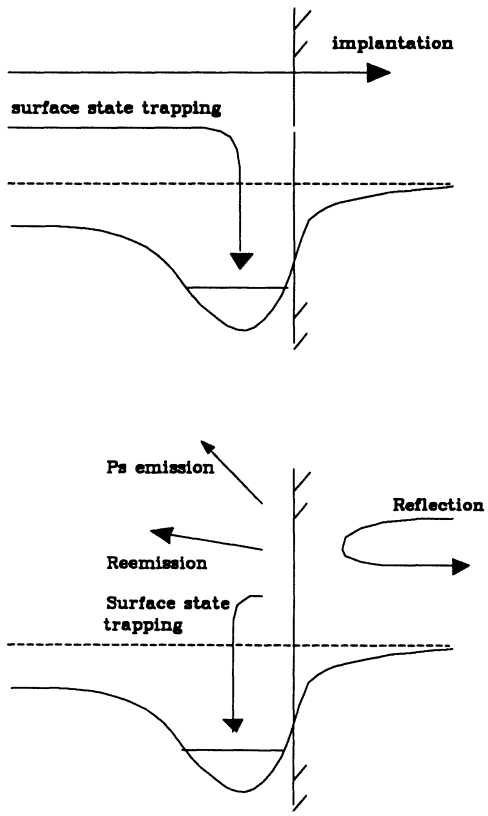

FIG. 1. Schematic picture of possible positron-surface processes (a) for positrons entering a metal and (b) for implanted positrons leaving the metal.

tures. Hence, either the positrons are reflected back into the bulk (i.e., the sticking coefficient is zero), or they are trapped into the image potential well (a sticking coefficient of unity). Unfortunately, it is very difficult to determine directly by experiment the fraction trapped into the surface state.[7] Hence, the question of whether the sticking coefficient of the positrons is zero or unity cannot be resolved by these measurements. The interpretation of this data is complicated by the need to make assumptions about the temperature dependence of the transition rate into the surface state ν_{ss}. Furthermore, the very different temperature dependence of Ps formation deduced from measurements at Ag(100) surfaces compared with measurements at Ag(111) surfaces creates additional difficulties for understanding these measurements. These issues are taken up in Sec. III C below.

The question of whether Ps sticks to metal surfaces is related to whether positrons stick to metal surfaces. This question has been examined in recent experiments of Mills *et al.*[8] and Martin, Bruinsma, and Platzman[9] which strongly suggest that in fact Ps sticks to metal surfaces at low temperatures. The calculations indicate[9] that the interaction of Ps with the surface is strong in the sense that the second-order perturbation theory for sticking seems to be inadequate.

There is also an interest in positron-surface sticking rates at nonzero positron energies. These are needed in many measurements of positron-surface phenomena. Baker, Touat, and Coleman[10] have measured branching ratios for positrons implanted into a Cu(110) surface at implantation energies of 5–40 eV. At such low values of the implantation energy, there is a significant probability that the positrons will return to the surface before they have thermalized. Thus an essential prerequisite for the interpretation of these data is an investigation of the surface-state transition rate $\nu_{ss}(E_i^+)$ and the probability per encounter that the positrons stick to the surface, $P_{ss}(E_i^+)$, for a range of E_i^+ exceeding thermal energies. Recently, McMullen and Stott[11] and Puska and Manninen[12] have shown that the trapping rates at vacancies in bulk metals may be considerably enhanced by p-wave scattering resonances. It has been suggested[10] that the increased trapping probabilities observed below an implantation energy of 20 eV may be consistent with an analogue for surfaces of this resonant trapping. We will address this suggestion in Sec. III D.

In this paper we have looked at the variation of the transition rate into the surface state, ν_{ss}, and the probability per surface encounter that the positrons stick to metal surfaces, P_{ss}, with the positron kinetic energy prior to trapping, E_i^+, for thermal and epithermal positrons. The (inelastic) process of trapping is assumed here to involve a transfer of energy to the electrons in the metal by the creation of electron-hole pairs. We have assumed a weak interaction between the positron and electrons in the metal and used first-order perturbation theory so that the process of trapping involves the creation of only one electron-hole pair. In this approach, the polarization of the electrons in the metal is included by statically screening the electron-positron Coulomb interaction.

The sticking probability $P_{ss}(E_i^+)$ for thermal positrons was first calculated by Neilson, Nieminen, and Szymański.[13] Our results differ from Ref. 13, and we have extended the theory (i) to cover the limit $E_i^+ \to 0$, (ii) to cover epithermal energies, (iii) to look at $\nu_{ss}(E_i^+)$, and (iv) to the case where the positron is trapped prior to implantation [Fig. 1(a)]. Note that the present results are more accurate than those published in a preliminary report on this work,[14] which followed the same procedure as in Ref. 13. In addition, we have looked at the variation of trapping rates with the positron work function, using tungsten as an example, and the extent to which the presence of He affects trapping rates into helium bubbles in metals, which is relevant to the interpretation of positron-lifetime measurements.[15]

The outline of the paper is as follows: Sec. II contains a short description of the formalism which is presented in more detail in the Appendix, Sec. III discusses the results, and Sec. IV is the conclusion.

II. METHOD

In the analysis of positron-surface interactions, a quantitative measure of the surface-state trapping is given by the transition rate to a bound state in a potential well at the surface per defect concentration ν_{ss}. The rate ν_{ss} enters into the boundary condition for the positron diffusion equation, see, e.g., Ref. 6. If we take L to be the linear dimension of the metal, with the metal surfaces located in the planes $z = -L$ and $z = 0$, we have

$$\nu_{ss} = 2L \sum_{p_{\|f}} \Lambda_{fi}, \tag{2.1}$$

where Λ_{fi} is the probability per unit time for the positron to make a transition from the initial state i to the final state f, and $p_{\|f}$ is the momentum parallel to the surface of the positron in the final state f.

We assume here that the energy lost by the positron in going from an extended state to a trapped state is given to an electron-hole pair. From the Fermi golden rule,

$$\Lambda_{fi} = (2\pi/\hbar) \sum_{\mathbf{k}} \sum_{\mathbf{q}} |M_{fi}|^2 f_{\mathbf{k}}(1 - f_{\mathbf{k}+\mathbf{q}}) \times \delta[E_{vf}^+ - E_{vi}^+ + \hbar^2(\mathbf{k}+\mathbf{q})^2/2m - \hbar^2\mathbf{k}^2/2m]. \tag{2.2}$$

Here $\mathbf{k}$ and $\mathbf{k}+\mathbf{q}$ are, respectively, the electron momenta before and after the transition, $f_{\mathbf{k}}(= 1$ for $k \leq k_F, = 0$ otherwise; where k_F is the Fermi wave vector) is the Fermi factor at 0 K, E_{vi}^+ (E_{vf}^+) is the positron initial (final) energy relative to the vacuum, m is the electron mass, and M_{fi} is the matrix element between initial and final system states ψ_i and ψ_f, respectively, for the perturbing potential V,

$$M_{fi} = \langle \psi_f | V | \psi_i \rangle. \tag{2.3}$$

Like Neilson, Nieminen, and Szymański,[13] we approximate ψ_i by the product of single-particle positron and electron wave functions; we assume a jellium model in

which the surface is represented by a uniform distribution of positive charge confined to the region $z \leq 0$, the electron states are given by the infinite barrier model, and the coupling potential V is a screened Coulomb potential, with the screening parameter μ set equal to a fixed fraction of μ_{TF} where the Thomas-Fermi screening parameter $\mu_{TF} = \sqrt{4k_F/\pi a_0}$ and a_0 is the Bohr radius. If the potential seen by the positron is approximated by an asymmetric square well, it is straightforward to calculate ν_{ss} from Eqs. (2.1)–(2.3) and full details of the calculation are given in the Appendix. Our matrix element contains an extra term compared with the expression given in Neilson, Nieminen, and Szymański,[13] as shown in the Appendix.

We have used the infinite barrier model although it would be possible to give the electron work function a more realistic value. We would not, however, expect this change to have a significant qualitative effect as all that would do would be to change the overlap between the $e+$ and $e-$ as is clear from Eq. (A5) in the Appendix. To go beyond the infinite barrier model would greatly increase the complexity of the calculations which would not appear to be justified in view of our neglect of positron-electron correlations.

We have also calculated the probability per surface encounter P_{ss}, which is related to ν_{ss} by[13,16]

$$P_{ss} = \nu_{ss}/(\hbar p_{zbi}/m), \tag{2.4}$$

where p_{zbi} is the z component of the initial wave vector of the positron in the bulk, defined such that

$$\hbar^2 p_{zbi}^2/2m = E_{vi}^+ + \phi^+. \tag{2.5}$$

ϕ^+ is the positron work function.

The above expression is only valid if $P_{ss} \ll 1$. For $P_{ss} \approx 1$, it should be replaced by a more general expression[16]

$$P_{ss} = 1 - \exp[-\nu_{ss}/(\hbar p_{zbi}/m)]. \tag{2.6}$$

We have used the simpler Eq. (2.4) for P_{ss} since the two definitions are equivalent for P_{ss} less than about 0.3, which holds in almost all the examples studied here.

The input parameters used in the calculations are presented in Table I and discussed in Sec. III A.

Our calculations have been done for the lowest bound state. We are not aware of any experimental evidence for trapping into higher bound states, perhaps because if they are only weakly bound the positron would be thermally desorbed and/or unstable to Ps formation.

III. RESULTS AND DISCUSSION

A. Parameters

The values adopted for the depth D and width w of the potential well seen by the positron are given in Table I, along with the positron work function ϕ^+, the radius r_s of a sphere containing one electron for the bulk metal, the binding energy of the trapped positron state E_b, and screening parameter μ.

D and w for the clean aluminium surface is chosen to make E_b approximately equal to the observed binding energy for an Al(100) surface, namely 2.80 eV.[20] There are no experimental measurements for E_b for the tungsten so we have used the same values for W and D as for the clean aluminium surface, given that for all the clean metal surfaces for which E_b has been measured, E_b lies between 2 and 3 eV.

TABLE I. Values of parameters used in the calculation—see text for definitions of the parameters.

	Al	W	Al + He
D	5.0 eV	5.0 eV	4.34 eV
w	2.5 Å	2.5 Å	2.5 Å
ϕ^+	−0.16 eV[a]	−3.0 eV[b]	−1.36 eV
r_S	1.10 Å[c]	1.24 Å[d]	1.10 Å[c]
E_b	3.02 eV	2.85 eV	2.4 eV
μ/μ_{TF}	0.6	0.6	0.6

[a]Gullikson and Mills (Ref. 17).
[b]Chen *et al.* (Ref. 18).
[c]Ashcroft and Mermin (Ref. 19).
[d]Assuming a lattice constant of 3.16 Å (Ref. 19), body-centered-cubic structure (Ref. 19), and a valence of 2.

The parameters for the surface of a helium bubble (denoted Al+He in Table I) are estimated assuming a helium density of $\sim 1 \times 10^{29}$ m^{-3}. Since there are no experimental measurements of E_b for the helium bubble surfaces, we have made estimates that take into account two effects: (i) the increase in the binding energy of the surface with respect to the vacuum of ≈ 0.6 eV (Ref. 21) and (ii) the lowering of positron energy outside the metal by $\approx$ 1.2 eV (Refs. 22 and 23) due to the helium. In our model, we incorporate these changes by decreasing ϕ^+ by 1.2 eV and decreasing D by 0.66 eV relative to clean aluminum.

We have set μ to a value below the bulk value μ_{TF} to take into account in an approximate way the fact that the electron density, at the metal-vacuum boundary, where the transitions take place, is lower than in the bulk. The value we have chosen is the same as that used by Neilson, Nieminen, and Szymański[13] for most of their calculations and is discussed in that reference. Since there is some arbitrariness about the value chosen, we have checked the sensitivity of our results to μ (see Fig. 9 and the discussion in Sec. III G).

B. Overview of the results

As indicated by Fig. 1, the positron can be trapped on entering the surface or, once implanted, on returning to the surface from the bulk. We have examined both these possibilities in our calculations of ν_{ss} and P_{ss} and our results are presented in Figs. 2–9. The inset on each panel indicates whether the positron is trapped before or after implantation. We have calculated ν_{ss} and P_{ss} assuming either that two-thirds of E_i^+ comes from motion in the surface plane (indicated by a diagonal arrow) or that the positron is moving perpendicular to the surface prior to trapping. Figures 2 and 3 give the calculated values of ν_{ss} for aluminum in two different energy ranges, Figs. 4 and 5 the corresponding results for P_{ss}. Figure 2(d) gives the

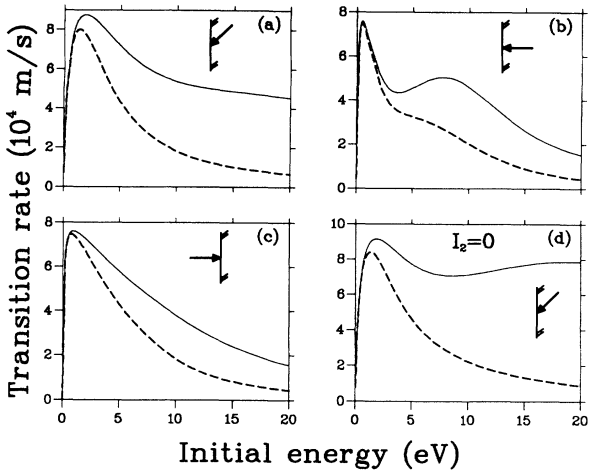

FIG. 2. The transition rate into the surface state ν_{ss} for aluminum as a function of the initial kinetic energy of the positron, E_i^+. Panels (a), (b), and (c) give results obtained from the complete model. The direction of motion of the positron prior to trapping is indicated by the insets: the diagonal arrow indicates that two-thirds of E_i^+ comes from motion in the surface plane. Panel (d) gives the results obtained if the contribution I_2 to the matrix element is set to zero. Solid and dashed lines correspond to different conditions on the final positron energy: $E_f^+ \leq E_i^+$ and $E_f^+ \leq 0$, respectively.

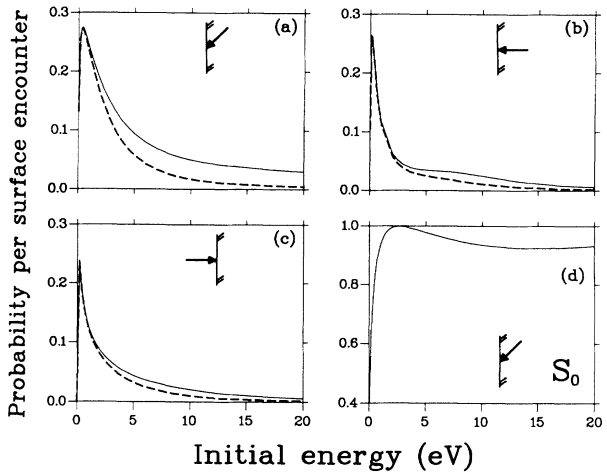

FIG. 4. Probability per surface encounter of trapping into the surface state P_{ss} for Al [panels (a), (b), and (c)]. The figure covers the same set of initial and final conditions as Fig. 2. Panel (d) shows the elastic transmission probability S_0.

results where we have set the extra term which we have found for the matrix element I_2 equal to zero. In Fig. 4(d) we have plotted the probability per encounter for transmission without scattering, $S_0 = p_{zvi} \mid T_v \mid^2 / p_{zbi}$.[13] Our predictions for ν_{ss} and P_{ss} for tungsten are shown in Fig. 6. The trapping rates at thermal energies for aluminum and tungsten and for voids and helium bubbles in aluminum are given in Figs. 7 and 8, respectively. Finally, in Fig. 9, we examine the effects on ν_{ss} and P_{ss} of varying μ.

In the figures the solid and dashed lines correspond to different maximum values imposed on the final-state positron energy. Since the final positron energy with respect to the vacuum is

$$E_{vf}^+ = \hbar^2 \mathbf{p}_{\|f}^2 / 2m - E_b, \tag{3.1}$$

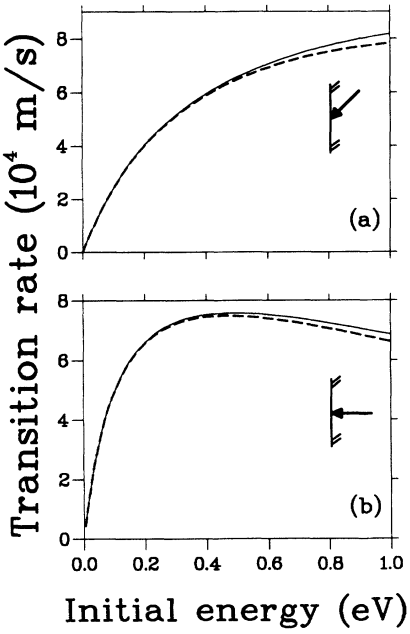

FIG. 3. The transition rate ν_{ss} for Al as a function of the initial kinetic energy of the positron E_i^+. Parameters as for Fig. 2, except for the energy range.

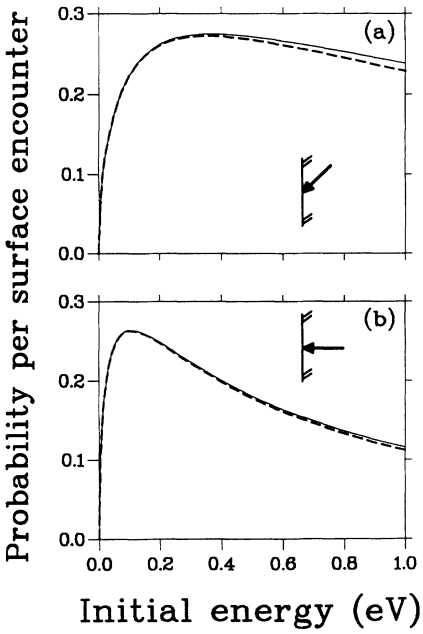

FIG. 5. Probability per surface encounter of trapping into the surface state P_{ss} for Al. Parameters as for Fig. 4, except for the energy range.

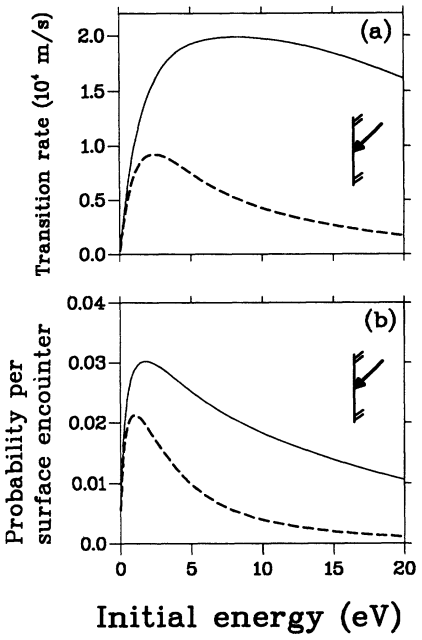

FIG. 6. The transition rate ν_{ss} (a) and probability per surface encounter P_{ss} (b) for trapping into the surface state for tungsten as functions of initial kinetic energy. The direction of motion of the positron prior to trapping is indicated by the insets. Solid and dashed lines correspond to different conditions on the final positron energy: $E_f^+ \leq E_i^+$ and $E_f^+ \leq 0$, respectively.

these maximum values impose limits on $p_{\|f}$. The solid curve corresponds to the restriction $E_{vf}^+ \leq E_{vi}^+$, i.e., the positron cannot gain energy as a result of the transition. For the dashed curve, we take $E_{vf}^+ \leq 0$. If E_{vf}^+ is positive,

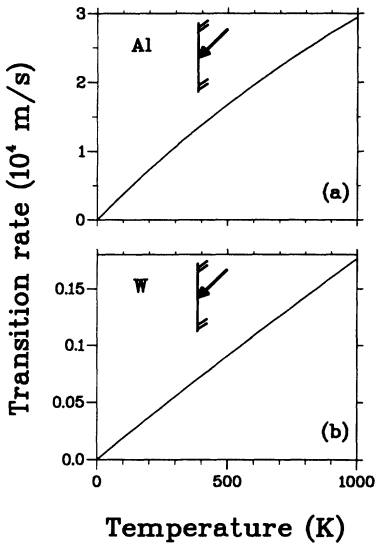

FIG. 7. The transition rate into the surface state ν_{ss} for positrons at thermal energy shown as a function of the temperature (a) for Al and (b) for W. The direction of motion of the positron prior to trapping is indicated by the insets. The condition $E_f^+ \leq E_i^+$ on the final energy is employed.

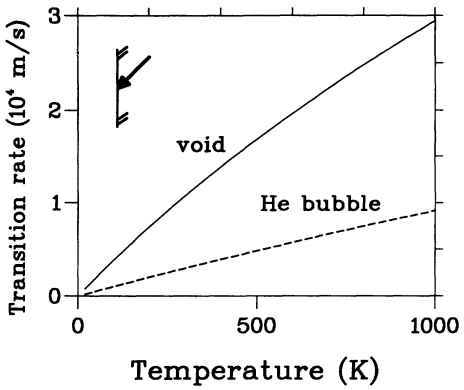

FIG. 8. The transition rate into the surface state ν_{ss} for positrons at thermal energy shown as a function of the temperature for trapping into voids and He bubbles in Al. The direction of motion of the positron prior to trapping is indicated by the insets. The condition $E_f^+ \leq E_i^+$ on the final energy is employed.

the final state may be unstable to free positron emission if the positron is scattered out of the surface by an elastic or quasielastic process. We do not attempt here to determine the fraction of positrons which scatter out of the surface compared with those that lose sufficient momentum parallel to the surface to end up near or at the ground state. We have therefore presented results for the extreme cases that positrons with sufficient kinetic

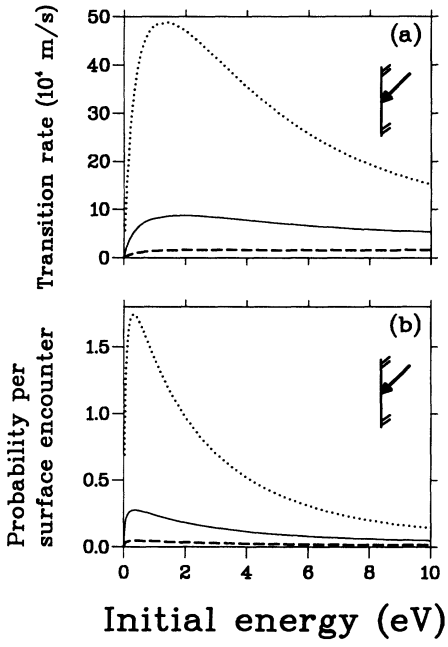

FIG. 9. The transition rate ν_{ss} (a) and probability per surface encounter P_{ss} (b) for trapping into the surface state for Al for three different values of the screening parameter: μ/μ_{TF}=0.3 (dotted lines), μ/μ_{TF}=0.6 (solid lines), and μ/μ_{TF}=1.0 (dashed lines). The direction of motion of the positron prior to trapping is indicated by the insets. The condition $E_f^+ \leq E_i^+$ on the final energy is employed.

energy parallel to the surface for $E_{vf}^{+} \geq 0$ slow down sufficiently fast that they are all trapped (solid curve), and that only the positrons with $E_{vf}^{+} \leq 0$ are trapped (dashed curve). For trapping into a cavity, the condition $E_{vf}^{+} \leq -\phi^{+}$ has been adopted to ensure that the positron cannot be scattered back into the metal.

C. Temperature dependence of the sticking coefficient

All the figures show that the sticking coefficient tends to zero at low temperatures and our results are consistent with the general result that within first-order perturbation theory, the sticking coefficient tends to zero as $(E_z)^{1/2}$. It is easy to see that with the wave functions we have used, Eq. (A12), that the matrix element must be zero in the limit $p_{zbi} \rightarrow 0$. It should be noted that this result holds for all surface potentials, including the more realistic ones where the potential seen by the positron outside the surface varies as $1/z$.[4,7]

Kong *et al.*[24] have recently calculated the transition rate into the surface state mediated by electron-hole pair excitation within first-order perturbation theory for positron temperatures of 50–700 K. They found that the rate is almost constant, although there is a weak linear dependence. This does not agree with our theory, see Fig. 7, and we do not have a satisfactory explanation for their results. It must be emphasized that the reflection coefficient is unity as the particle energy tends to zero regardless of the sign of the work function. Hence, if the positron-surface coupling is weak, the sticking coefficient will be zero for positive work function surfaces as well as for negative work function surfaces. Huttunen *et al.*[7,24] find that the Ps yield remains high for the Ag(100) surface even at the lowest attainable temperature of 20 K and above that temperature shows no sign of tending towards zero as the temperature is reduced. They suggest this is due to the fact that this surface has a positive positron work function, arguing that reflection is less important for such surfaces. These measurements are hard to reconcile with the notion that the sticking coefficient is zero or unity. For weak positron-surface coupling, the positron will be reflected back into the bulk and the overlap with the tail of the electron density at the surface where Ps can be formed becomes vanishingly small at low temperatures so that no Ps should be formed. If, however, the coupling is strong, all the positrons will be trapped into the surface state at low temperatures and so again no Ps should be observed. We believe that a fresh look must be taken at the measurements for the Ag(100) and Ag(111) surfaces which takes these points into account.

We have also looked at ν_{ss} and P_{ss} for tungsten which is widely used as a moderator material. Complications arising from tungsten being a transition metal, for which the jellium model is not strictly applicable, have been ignored to give order of magnitude estimates. This has the advantage that we can see directly changes in ν_{ss} and P_{ss} arising simply from changing the positron work function. Figures 6 and 7 show that the results are similar to those for Al, except that ν_{ss} and P_{ss} are considerably less for tungsten. This is a matrix element effect, arising from the reduced overlap between initial and final states for tungsten due to the increased height of the potential step at the surface. Thus we predict strong variations of ν_{ss} and P_{ss} with ϕ^{+}.

D. Epithermal positrons and branching ratios

The strong dependence of ν_{ss} and P_{ss} on E_i^{+} arises from three effects: (i) the extent to which the positron is reflected off the surface (on entering) or into the bulk (on leaving), (ii) the variation of the matrix element with E_i^{+}, and (iii) the phase space available to the trapped positron and excited electron-hole pair. It is clear by comparing Figs. 3 and 5 with Fig. 4(d) that the variation of ν_{ss} and P_{ss} with E_i^{+} for E_i^{+} less than 2 eV is dominated by transmission and reflection at the potential well boundaries but above this energy the matrix element and phase space considerations dominate causing a rapid decrease in the trapping rates and probabilities. The chief difference that inclusion of some initial in-plane momentum makes to the final results is to change the energy scale in proportion to the fraction of kinetic energy available perpendicular to the surface.

Our results may be compared with the branching ratio measurements of Baker, Touat, and Coleman,[10] who measured the branching ratios for 0–40-eV positrons incident on Cu(110) surfaces at room temperature. The branching ratios are denoted ε_{e^+}, $\varepsilon_{\mathrm{Ps}}$, and ε_{ss}, for the channels of emission as free positrons, Ps formation, and trapping into the surface (or bulk annihilation), respectively. When making the comparison, one has to consider both the possibility that positrons from a beam may be trapped into the surface state before they penetrate the surface and the possibility that they are trapped after they diffuse back to the sample surface once implanted (Fig. 1). For implanted positrons, the trapping probability depends on the energy distribution of the positrons that return to the surface. Simulations of positron slowing down at implantation energies in the range 5–50 eV (Ref. 25) show that the distribution of positrons as a function of their kinetic energy perpendicular to the surface only depends weakly on the implantation energy in this energy range. This is due to the fact that the initial slowing down is extremely rapid and takes place over a distance of ~ 10 Å, implying that the energy distribution is governed by the positron motion at energies below 5 eV. Thus, since bulk annihilations can be ignored, ε_{ss} for implanted positrons is independent of the implantation energy and is close to ε_{ss} for a thermalized positron.

However, for positrons trapped prior to implantation, E_i^{+} is equal to the implantation energy and there is a single encounter with the surface so that the trapping probability is equal to $P_{ss}(E_i^{+})$, which is presented in Fig. 4(c). Our results in Fig. 2(c) show a decrease in $P_{ss}(E_i^{+})$ from about 10% to zero over the range 2–20 eV. The measurements of Baker, Touat, and Coleman[10] show a decrease in ε_{ss} from about 0.35 at an implantation energy of about 2 eV to 0.25 at an implantation energy of about 20 eV. This decrease must be due to positrons

trapped prior to implantation, with a constant contribution of 0.25 associated with positrons that have entered the metal and thermalized before returning to the surface. The fact that we can satisfactorily explain the experimental data gives support to the idea that positrons do couple weakly to the surface.

Our calculations should be relevant to any experiments where the possibility of epithermal trapping arises. We intend to pursue this question by coupling our predictions for trapping rates with predictions of positron slowing down using a Monte Carlo simulation code that has shown some success in predicting positron implantation profiles.[26] Note that P_{ss} cannot be equated to ε_{ss} for implanted positrons. The reason is that the latter is determined by the total probability for the positrons either to be trapped or to annihilate in the bulk after multiple encounters with the surface. Hence it is necessary to calculate the probability per surface encounter for positrons to form Ps and to be reemitted as free positrons as well.

E. Surface resonances

Baker, Touat, and Coleman[10] suggested that their observed variation in ε_{ss} with the implantation energy for clean surfaces at room temperature might be explained by an analogue to the centrifugal barrier that leads to trapping resonances for vacancies. We have looked at the possibility that there might be some variation in the trapping rate with E_i^+ due to variations in the transmission coefficient T_v, leading to resonances of the type seen in simple one-dimensional calculations of transmission of quantum particles across rectangular wells; see, for example, Ref. 27. These resonances are due to matching of the nodes of the wave function with the well edges. This possibility can be discounted due to the fact that the variations in the transmission rate from this effect are small—see Fig. 4(d)—and are swamped by the variation with E_i^+ of other factors affecting the matrix element. With hindsight, this result is readily understood from the different symmetry (i.e., cylindrical rather than spherical) appropriate to this problem.

The fact that we do not find resonances in our calculation of ν_{ss} does not preclude them altogether. Positron analogues of the electron surface resonances of crystals[28] have been discussed by Jennings and by Jennings and Neilson.[29] Such resonances would be seen in low-energy electron diffraction (LEED) and low-energy positron diffraction (LEPD) in the form of interference features below the emergence thresholds in the specularly reflected beam. As described in Ref. 28, they arise when the electron (or positron) is temporarily trapped into an intermediate state in which the total energy of the electron (or positron) is positive, but the wave function normal to the surface is the bound state in the image potential well. The net transition is elastic, unlike the process studied in this paper which is strongly inelastic, so the existence of these surface resonances is not inconsistent with our results.

F. Voids

To explain the experimental measurements on voids[30,31] showing that positrons do annihilate from the surface state in the voids even for sample temperatures approaching 0 K, we have calculated thermalization rates using the Boltzmann equation and demonstrated[32] that the positrons do not fully thermalize before being trapped. Nonthermal trapping then ensures a finite trapping probability.

Our transition rates at room temperature, $\sim 10^4\ \mathrm{m\,s^{-1}}$ (Figs. 2 and 8), are within an order of magnitude of trapping rates deduced from experiment[30,31] which gives us some confidence in the validity of our model, despite uncertainties over the value of μ. In fact, our weak-coupling model overestimates ν_{ss}. If the coupling were strong, the predicted transition rate would be even higher, leading to worse agreement with the experimental values. In Ref. 31 the positron initial state was approximated by a plane wave orthogonalized to the bound state which neglects reflection of the positron off the potential well at the void surface. Our results show that it is important to include this effect to obtain the correct energy dependence at low energies.

The conclusion that we can draw from Fig. 8, which compares trapping rates for voids and helium bubbles, is that trapping rates into the bubbles do depend strongly on the helium density, n_{He}. This result is contrary to assumptions made when interpreting measurements on samples with helium bubbles.[15] The analysis procedure widely used assumes that the specific trapping rate depends on the bubble radius but not on n_{He}. Our result implies that the dependence on n_{He} should be taken into account in cases where the trapping rate is governed by the transition rate into the bubble rather than diffusion to the bubble, usually true for small bubbles at high concentrations.[33]

G. Screening effects

It is useful to see the effect on the results of changing the screening parameter μ. Like Ref. 13, we find that ν_{ss} and P_{ss} are sensitive to this value, as is clearly shown in Fig. 9 where ν_{ss} and P_{ss} are shown as a function of energy. Our results show that ν_{ss} and P_{ss} possess the same overall dependence on energy regardless of the value of μ but that the maximum values differ by an order of magnitude, consistent with Ref. 13. This result can easily be understood from the fact that the more strongly the coupling potential is screened, the weaker it is, significantly affecting the matrix element. In order to properly treat screening effects at the surface one would have to consider nonlocal positron-electron correlation effects in a nonhomogeneous electron system.

IV. CONCLUSION

In this paper we have analyzed a number of experiments that look at positron-surface sticking rates within

a model that assumes that positrons couple weakly to the surface so that first-order perturbation theory is valid. Our calculations provide strong arguments that fresh interpretation is necessary for experimental data on trapping rates for thermalized positrons into the surface state at low temperatures[7] and provide explanations for data on epithermal positron trapping at low implantation energies[10] and into voids.[30] We have found that trapping rates are not affected by surface resonances but that they are sensitive to the positron work function, and in the case of helium bubbles they are sensitive to the presence of the helium.

Comparisons of our model with available experimental data on trapping rates for positrons into the surface state[30,10] show that the positron-surface coupling must indeed be weak. This in turn supports our prediction that ν_{ss} and P_{ss} and hence the positron-surface sticking coefficient vanish as the kinetic energy of the positron goes to zero. So far, there has been no direct observation of this. We hope that this paper may stimulate further experiments in this area, particularly with pulsed beams that can be used to measure positron lifetimes and hence identify whether the positrons annihilate in the bulk or at the surface. It would also be of value to take a fresh look at existing experiments in the light of the predictions that the sticking coefficient should either be zero or unity at zero temperature.

ACKNOWLEDGMENTS

We would like to thank Paul Coleman and Risto Nieminen for useful discussions. K.O.J. would like to thank the Commission of the European Communities for a Research Grant under Contract No. SCI-0163 and A.B.W. would like to thank the University of New South Wales, where some of this work was done.

APPENDIX

Below, we give a full derivation and expressions for ν_{ss} within the assumptions discussed in Sec. II. Within the jellium model of the surface, the electron and positron wave functions are given by

$$\psi_i^-(\mathbf{r}^-) = \sqrt{(2/\Omega)}\exp[i\mathbf{k}\cdot\mathbf{r}_\parallel^-]\psi_{zi}^-(z^-), \tag{A1}$$

$$\psi_f^-(\mathbf{r}^-) = \sqrt{(2/\Omega)}\exp[i(\mathbf{k}+\mathbf{q})\cdot\mathbf{r}_\parallel^-]\psi_{zf}^-(z^-), \tag{A2}$$

and

$$\psi_i^+(\mathbf{r}^+) = \frac{\exp[i\mathbf{p}_{\parallel i}\cdot\mathbf{r}_\parallel^+]}{L}\psi_{zi}^+(z^+), \tag{A3}$$

$$\psi_f^+(\mathbf{r}^+) = \frac{\exp[i\mathbf{p}_{\parallel f}\cdot\mathbf{r}_\parallel^+]}{L}\psi_{zf}^+(z^+), \tag{A4}$$

where the subscript $\parallel$ denotes vectors parallel to the surface.

Using our model, the matrix element is given by

$$M_{fi} = \int d\mathbf{r}^+ \int d\mathbf{r}^- \psi_f^{+*}(\mathbf{r}^+)\psi_f^{-*}(\mathbf{r}^-)\frac{e^2\exp(-\mu|\mathbf{r}^+-\mathbf{r}^-|)}{4\pi\epsilon_0|\mathbf{r}^+-\mathbf{r}^-|}\psi_i^+(\mathbf{r}^+)\psi_i^-(\mathbf{r}^-)$$
$$= \frac{e^2}{4\pi\epsilon_0}\frac{8\pi^2}{L^4}\delta(\mathbf{p}_{\parallel i}-\mathbf{p}_{\parallel f}-\mathbf{q}_\parallel)\int dz^+\psi_{zf}^{+*}(z^+)\psi_{zi}^+(z^+)\int dz^-\psi_{zf}^{-*}(z^-)\psi_{zi}^-(z^-)\int dt_z\frac{\exp[-it_z(z^+-z^-)]}{t_z^2+q_\parallel^2+\mu^2}. \tag{A5}$$

Using the infinite barrier model for the electrons, with the barrier at $z=0$,

$$\psi_{zi}^-(z^-) = \sqrt{(2/L)}\sin[k_z z^-]\Theta(-z^-) \tag{A6}$$

and

$$\psi_{zf}^-(z^-) = \sqrt{(2/L)}\sin[(k_z+q_z)z^-]\Theta(-z^-). \tag{A7}$$

Here $\Theta(x)$ is the unit step function.

From Eqs. (A1)–(A7), we get after some algebra,

$$M_{fi} = \delta(\mathbf{p}_{\parallel i}-\mathbf{p}_{\parallel f}-\mathbf{q}_\parallel)\frac{e^2}{4\pi\epsilon_0}\frac{16\pi^3}{L^5}(I_1+\tfrac{1}{2}I_2), \tag{A8}$$

where

$$I_1 = \int_{-\infty}^0 dz^+\psi_{zf}^{+*}(z^+)\psi_{zi}^+(z^+) \times\left[\frac{\cos(q_z z^+)}{q_z^2+q_\parallel^2+\mu^2}-\frac{\cos[(2k_z+q_z)z^+]}{(2k_z+q_z)^2+q_\parallel^2+\mu^2}\right] \tag{A9}$$

and

$$I_2 = \int_{-\infty}^\infty dz^+\psi_{zf}^{+*}(z^+)\psi_{zi}^+(z^+) \times\mathrm{sign}(z^+)\exp(-\sqrt{q_\parallel^2+\mu^2}|z^+|) \times\left[\frac{1}{q_z^2+q_\parallel^2+\mu^2}-\frac{1}{(2k_z+q_z)^2+q_\parallel^2+\mu^2}\right]. \tag{A10}$$

Note that this matrix element differs from the expression given in Eq. (8) of Ref. 13 (which was also used in Ref. 14), in that the integration limits prescribed for I_1 are different and there is an additional term I_2. These differences arise from taking full account of the fact that the electron wave functions are zero outside the surface of the metal. In practice the term I_2 have little effect on our numerical results. In our previous results there is a factor missing, π in Ref. 13 and 2 in Ref. 14.

Like Ref. 13, we have represented the potential seen by the positron at a surface as a simple square well,

$$V^+(z^+) = \begin{cases} -\phi^+ & \text{for } z^+ \le 0 \\ -D & \text{for } 0 \le z^+ \le w \\ 0 & \text{for } w \le z^+. \end{cases} \tag{A11}$$

If the positrons are leaving the surface,

$$\psi_i^+(z^+) = \begin{cases} [\exp(ip_{zbi}z^+) + R_b \exp(-ip_{zbi}z^+)]/W_{li} & \text{for } z^+ \le 0 \\ [T_w \exp(ip_{zwi}z^+) + R_w \exp(-ip_{zwi}z^+)]/W_{li} & \text{for } 0 \le z^+ \le w \\ T_v \exp(ip_{zvi}z^+)/W_{li} & \text{for } w \le z^+. \end{cases} \tag{A12}$$

Here p_{zbi}, p_{zwi} and p_{zvi} are, respectively, the initial wave vectors of the positron in the bulk metal, well, and vacuum, R_b (R_w) the reflection amplitudes for the positron in the bulk metal (well), T_w (T_v) the transmission amplitudes for the positron in the well (vacuum), and W_{li} is the normalization constant for $\psi_{zi}^+(z^+)$,

$$W_{li}^2 = L(1 + |R_b|^2 + |T_v|^2). \tag{A13}$$

If the positrons are entering the surface,

$$\psi_{zi}^+(z^+) = \begin{cases} T_b \exp(ip_{zbi}z^+)/W_{ei} & \text{for } z^+ \le 0 \\ [T_w \exp(ip_{zwi}z^+) + R_w \exp(-ip_{zwi}z^+)]/W_{ei} & \text{for } 0 \le z^+ \le w \\ [\exp(ip_{zvi}z^+) + R_v \exp(-ip_{zvi}z^+)]/W_{ei} & \text{for } w \le z^+, \end{cases} \tag{A14}$$

where T_b is the transmission coefficient for the positrons in the bulk metal and W_{ei} is the normalization constant for $\psi_{zi}^+(z^+)$:

$$W_{ei}^2 = L(1 + |R_v|^2 + |T_b|^2). \tag{A15}$$

The final result for the transition rate is

$$\nu_{ss} = C \int_0^{p_{\|f}^{\max}} dp_{\|f} \int_0^{\pi} \frac{d\phi_{\|f}}{q_{\|f}} \int_0^{k_F} dk_z \int_{q'_{zl}}^{q'_{zu}} dq'_z [\Delta_2 \theta(\Delta_2) - \Delta_1 \theta(\Delta_1)] \left| I_1 + \frac{I_2}{2} \right|^2, \tag{A16}$$

where $p_{\|f}^{\max}$ is obtained from the conditions $E_{vf}^+ \le E_{vi}^+$ or $E_{vf}^+ \le 0$ (discussed in Sec. III B),

$$\Delta_1 = \sqrt{k_F^2 - k_z^2 - \tilde{K}_{0\|}^2 - \alpha^2}, \tag{A17}$$

$$\Delta_2 = \sqrt{\Delta_1^2 + \alpha^2}, \tag{A18}$$

$$\tilde{K}_{0\|} = \sqrt{\frac{\alpha^2 - q_\|^2 - q_z^2 - 2k_z q_z}{2q_\|}}, \tag{A19}$$

$$q'_z \equiv q_z + k_z, \tag{A20}$$

$$q'_{zl} = \sqrt{\alpha^2 - q_\|^2 + k_z^2 - 2q_\|(k_F^2 - k_z^2)^{1/2}}, \tag{A21}$$

$$q'_{zu} = \sqrt{q_{zl}'^2 + 4q_\|(k_F^2 - k_z^2)^{1/2}}. \tag{A22}$$

If the positron is leaving the metal,

$$\alpha^2 = (2m/\hbar^2)(E_b + E_{kzi} + |\phi^+|) - p_{\|f}^2 \tag{A23}$$

and

$$C = \frac{\hbar}{ma_0^2} \frac{32}{\pi^3}. \tag{A24}$$

If the positron is entering the metal, W_{ei} replaces W_{li} and

$$\alpha^2 = (2m/\hbar^2)(E_b + E_{kzi}) - p_{\|f}^2. \tag{A25}$$

[1] T. Martin and R. Bruinsma, Phys. Rev. B **41**, 3172 (1990).
[2] T. Martin and R. Bruinsma, Phys. Rev. B **40**, 8290 (1989).
[3] T. Martin, R. Bruinsma, and P.M. Platzman, Phys. Rev. B **39**, 12 411 (1989).
[4] T. Martin, R. Bruinsma, and P.M. Platzman, Phys. Rev. B **38**, 2257 (1988).
[5] N. Bigelow, Phys. World **3**, 20 (1990).
[6] D.T. Britton, P.A. Huttunen, J.A. Mäkinen, E. Soininen, and A. Vehanen, Phys. Rev. Lett. **62**, 2413 (1989).
[7] P. Huttunen J.A. Mäkinen, D.T. Britton, E. Soininen, and A. Vehanen, Phys. Rev. B **42**, 1560 (1990).
[8] A.P. Mills, Jr., E.D. Shaw, M. Leventhal, P.M. Platzman, R.J. Chichester, D.M. Zuckerman, T. Martin, R. Bruinsma, and R.R. Lee, Phys. Rev. Lett. **66**, 735 (1991).
[9] T. Martin, R. Bruinsma, and P.M. Platzman, Phys. Rev. B **43**, 6466 (1991)
[10] J.A. Baker, M. Touat, and P.G. Coleman, J. Phys. C **21**, 4713 (1988).
[11] T. McMullen and M.J. Stott, Phys. Rev. B **34**, 8985 (1986).
[12] M.J. Puska and M. Manninen, J. Phys. F **17**, 2235 (1987).
[13] D. Neilson, R.M. Nieminen, and J. Szymański, Phys. Rev. B **33**, 1567 (1986).
[14] A.B. Walker and K.O. Jensen, in *Positron Beams for Solids and Surfaces*, edited by Peter J. Schultz, Guiti R. Massoumi, and Peter J. Simpson, AIP Conf. Proc. No. 218 (AIP, New York, 1990), p. 98.
[15] K.O. Jensen, M. Eldrup, B.N. Singh, and M. Victoria, J. Phys. F **18**, 1069 (1988).
[16] Z.W. Gortel and J. Szymański, Phys. Lett. A **147**, 59 (1990); Phys. Rev. B **43**, 1919 (1990).
[17] E.M. Gullikson and A.P. Mills, Phys. Rev. B **36**, 8777 (1987).
[18] D.M. Chen, K.G. Lynn, R. Pareja, and B. Nielsen, Phys. Rev. B **31**, 4123 (1985).
[19] N.W. Ashcroft and N.D. Mermin, *Solid State Physics* (Holt, Rinehart and Wilson, New York, 1976).
[20] P. Schultz and K.G. Lynn, Rev. Mod. Phys. **60**, 701 (1988).
[21] K.O. Jensen and R.M. Nieminen, Phys. Rev. B **36**, 8219 (1987).
[22] P. Hautojärvi, K. Rytsölä, P. Tuovinen, A. Vehanen, and P. Jauho, Phys. Rev. Lett. **38**, 842 (1977).
[23] H.E. Hansen, R.M. Nieminen, and M.J. Puska, J. Phys. F **14**, 1299 (1977).
[24] Y. Kong, R.M. Nieminen, P.A. Huttunen, A. Vehanen and J. Mäkinen, in *Positron Beams for Solids and Surfaces* (Ref. 14), p. 91.
[25] K.O. Jensen and A.B. Walker (unpublished).
[26] J.A. Baker, N.B. Chilton, K.O. Jensen, A.B. Walker, and P.G. Coleman, Appl. Phys. Lett. **59**, 2962 (1991).
[27] L.I. Schiff, *Quantum Mechanics* (McGraw-Hill, London, 1968).
[28] E.G. McRae, Rev. Mod. Phys. **51**, 541 (1979).
[29] P.J. Jennings, Surf. Sci. **198**, 180 (1988); P.J. Jennings and D. Neilson, Solid State Commun. **65**, 649 (1988).
[30] K.O. Jensen, M. Eldrup, S. Linderoth, and H.J. Evans, J. Phys. Condens. Matter. **2**, 2081 (1990).
[31] R.M. Nieminen, J. Laakkonen, P. Hautojärvi, and A. Vehanen, Phys. Rev. B **19**, 1397 (1979).
[32] K.O. Jensen and A.B. Walker, J. Phys. Condens. Matter **4**, 1973 (1992).
[33] M. Eldrup and K.O. Jensen, Phys. Status Solidi A **102**, 145 (1987).